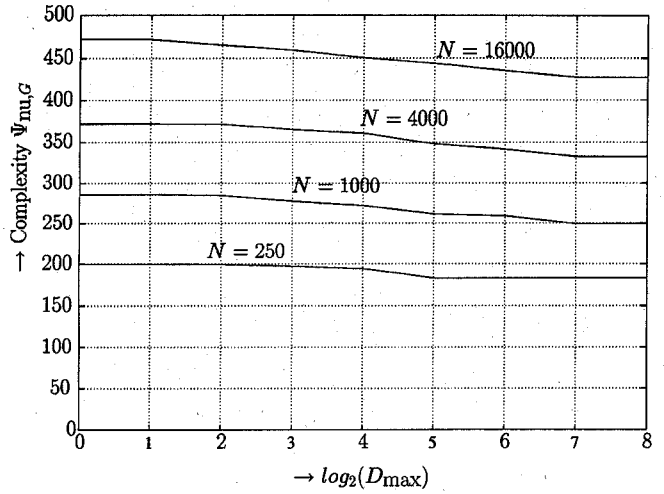

Fig. 11. Complexity of NU-PBFDAF.

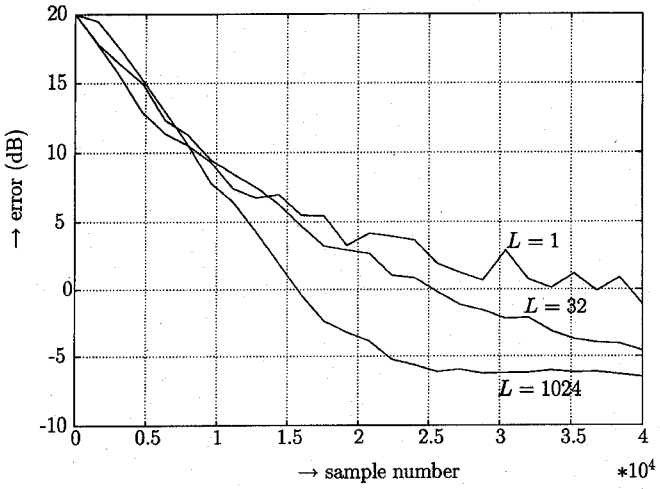

Fig. 12. Convergence for different update FFT lengths L.

output error is defined by

$$\text{error}[k] = 10 \cdot \log_{10}\left(\frac{\mathcal{E}\{(e[k]-\hat{e}[k])^2\}}{\mathcal{E}\{(s[k])^2\}}\right). \quad (43)$$

This error is independent on the way of realizing the filter part of the algorithm. The convergence properties of NU-PBFDAF algorithm will be equal to the properties of a DPBFDAF algorithm with an equal partition factor and block length in the update part. The two most important parameters for the behavior of the error are α and L (the update part FFT length). In Fig. 12, the dependency of the error on L is depicted. For increasing L the convergence behavior becomes better.

IV. Conclusions

The introduced new method for fast real-time convolution in the frequency domain by using nonuniform partitioning reduces the required number of real multiplications compared with a traditional approach using uniform partitioning.

For the case of adaptive filtering, the computational complexity can be reduced enormously, compared the traditional approaches in DPBFDAF. Complexity becomes almost independent on the maximum allowable delay. As a rule of thumb, the number of real multiplications per sample equals approximately $45 \cdot \log_2(N) - 160$, with N the number of filter coefficients.

References

[1] A. V. Oppenheim and R. W. Shafer, *Digital Signal Processing.* Englewood Cliffs, NJ: Prentice-Hall, 1975.

[2] E. R. Ferrara, "Fast implementation of LMS adaptive filter," *IEEE Trans. Acoust., Speech, Signal Processing,* vol. ASSP-28, pp. 474–475, Aug. 1980.

[3] G. A. Clark, "Block implementation of adaptive digital filters," *IEEE Trans. Acoust., Speech, Signal Processing,* vol. ASSP-29, no. 3, pp. 744–752, June 1981.

[4] M. R. Asharif *et al.*, "Frequency domain noise canceller: Frequency bin adaptive filtering," in *Proc. ICASSP,* Tokyo, Sept. 1986, pp. 2219–2222.

[5] J. S. Soo and K. K. Pang, "A new structure for block FIR adaptive digital filters," in *Proc. IEEE Conf.,* Sydney, Australia, Sept. 1987, pp. 364–367.

[6] P. C. W. Sommen, "Partitioned frequency domain adaptive filters," in *Proc. Asilomar Conf. Signals Syst.,* Pacific Grove, CA, 1989, pp. 676–681.

[7] G. P. M. Egelmeers and P. C. W. Sommen, "Relation between reduced dimension time and frequency domain adaptive algorithm," in *Signal Processing VI, Proc. EUSIPCO 1992,* Brussels, Belgium, Aug. 1992, pp. 1065–1068.

[8] G. P. M. Egelmeers, "Decoupling of partition factors in partitioned block FDAF," in *Proc. ECCTD 1993,* Davos, Switzerland, Aug. 1993, pp. 323–328.

[9] G. P. M. Egelmeers and P. C. W. Sommen, "A new method for efficient convolution in frequency domain by nonuniform partitioning," in *Proc. EUSIPCO 1994,* Edinburgh, Scotland, Sept. 1994, pp. 1030–1033.

Wigner-Based Formulation of the Chirplet Transform

Richard G. Baraniuk and Douglas L. Jones

***Abstract*— Using the Wigner distribution, we derive and analyze a matrix formulation for the chirplet transform, a signal analysis tool that generalizes the wavelet and short-time Fourier transforms. The formulation expresses the translations, scalings, and shears of the chirplet transform in terms of affine matrix transformations on the time-frequency plane. Our approach leads naturally to several new signal transforms, which we derive, analyze, and extend.**

I. Introduction

The short-time Fourier transform (STFT) and the continuous wavelet transform (WT) are time-frequency signal representations that indicate the time-varying frequency content of one-dimensional (1-D) signals [1], [2]. Both transforms have proven useful in a wide range of applications, including the analysis of radar, sonar, and geophysical signals, and the analysis and coding of speech signals and images.

Manuscript received March 1, 1996; revised June 18, 1996. This work was supported by the National Science Foundation under Grants MIP 90-12747 and MIP 94-57438, by the Office of Naval Research under Grant N00014-95-1-0849, and by the Joint Services Electronics Program under Grant N00014-90-J-1270. The associate editor coordinating the review of this manuscript and approving it for publication was Dr. Jose Moura.

R. G. Baraniuk is with the Department of Electrical and Computer Engineering, Rice University, Houston, TX 77251-1892 USA (e-mail: richb@rice.edu).

D. L. Jones is with the Coordinated Science Laboratory, University of Illinois, Urbana, IL 61801 USA (e-mail:d-jones@csl.uiuc.edu).

Publisher Item Identifier S 1053-587X(96)09061-7.

The STFT

$$(\mathbf{C}^{\text{stft}}s)(t, f) = \int s(u)g^*(u-t)e^{-j2\pi fu}\,du \tag{1}$$

projects the signal s onto the set of functions $\{g(u-t)e^{j2\pi fu}\}_{(t,f)\in\mathbb{R}^2}$ formed by shifting and modulating a lowpass window function g. Shifts and modulations translate the essential support of the window in time-frequency (see Fig. 1(a)). The WT

$$(\mathbf{C}^{\text{wt}}s)(t, a) = e^{-a/2}\int s(u)g^*[e^{-a}(u-t)]\,du \tag{2}$$

projects s onto the set of functions $\{e^{-a/2}g[e^{-a}(u-t)]\}_{(t,a)\in\mathbb{R}^2}$ formed by shifting and scaling a bandpass wavelet function g. Shifts and scale changes translate and scale the support of the wavelet in time-frequency (see Fig. 1(b)).

The STFT and WT perform best for signals whose characteristics match the time-frequency transformation employed in their analysis. The time-frequency translations of the STFT match signals having a constant-bandwidth behavior (frequency-shift keying signals, for example), whereas the time translations and scalings of the WT match signals having a proportional-bandwidth behavior (Doppler-shifted transients and fractal signals, for example). While the signals encountered in many applications are often approximately constant- or proportional-bandwidth, for many signals neither transform is suitable. Examples include dispersive or chirping signals that are matched only by chirping functions that slant in time-frequency.

The *chirplet transform* was developed to fill this need for a class of signal representations more general than the STFT and WT [3]–[8]. This transform projects the signal onto analysis functions that *shear* and *rotate* in time-frequency, in addition to translate and scale (see Fig. 1(c)). Besides providing a unifying framework for studying the STFT and WT, the chirplet transform provides a systematic method for designing new representations with properties useful for certain types of signals.

A Brief History of Chirplets: The chirplet transform has appeared under a number of different guises, first in optics (its origins can be traced back as far as Fresnel in the 1820's [9]) and quantum mechanics, and then in signal analysis. An essentially identical transform has been independently introduced and developed by several authors, each with a different emphasis. In quantum mechanics, Grossman and Paul studied the affine coherent states [3]. In signal theory, Berthon emphasized radar applications [4], Mann and Haykin considered "physical considerations" and coined the term *chirplet* [5], [6], and Baraniuk and Jones introduced a Wigner distribution interpretation [7], [8]. Closely related work has included the study of shear transformations in the ambiguity domain by Papoulis [10] and in the time-frequency domain by Janssen [11] and Jones and Parks [12], Schempp's study of the same using harmonic analysis [13], and Torrésani's time-frequency-scale "wavelet packet" transform [14].

In this correspondence, we present a framework for the chirplet transform that provides a reinterpretation of [3]–[8] and yields new insight into its properties. Our formulation expresses the translations, scalings, and shears of the chirplet transform in terms of affine matrix transformations on the time-frequency plane. In Section II, we use the Wigner distribution to derive the transform. The chirplet concept leads to several new signal transforms, which we derive, analyze, and extend in Section III. We close in Section IV with a discussion and conclusions.

II. Wigner-Based Formulation of the Chirplet Transform

A. Affine Time-Frequency Transformations

The basic transformations underlying both STFT and WT analyses can be neatly summarized in terms of matrix transformations on the time-frequency plane (recall Fig. 1). In the STFT (1), setting the analysis parameters to (t, f) translates the feature of the window g at time τ' and frequency ν' to the new location

$$\begin{bmatrix}\tau\\ \nu\end{bmatrix} = \begin{bmatrix}1 & 0\\ 0 & 1\end{bmatrix}\begin{bmatrix}\tau'\\ \nu'\end{bmatrix} + \begin{bmatrix}t\\ f\end{bmatrix}. \tag{3}$$

In the WT (2), setting the analysis parameters to (t, a) translates and scales the feature of the wavelet g at time τ' and frequency ν' to

$$\begin{bmatrix}\tau\\ \nu\end{bmatrix} = \begin{bmatrix}e^{a} & 0\\ 0 & e^{-a}\end{bmatrix}\begin{bmatrix}\tau'\\ \nu'\end{bmatrix} + \begin{bmatrix}t\\ 0\end{bmatrix}. \tag{4}$$

The chirplet transform unifies and extends these transforms through the more general affine transformation

$$\begin{bmatrix}\tau\\ \nu\end{bmatrix} = A\begin{bmatrix}\tau'\\ \nu'\end{bmatrix} + b, \qquad |A| = 1 \tag{5}$$

with A a 2×2 unimodular matrix and b a 2×1 vector. This transformation allows *shears* and *rotations* of the analyzing window/wavelet on the time-frequency plane [10]–[13].

B. Wigner Distribution

Before we can relate the analysis transformation (5) to operations on an analysis function, we must make precise the correspondence between a function and its representation on the time-frequency plane. The Wigner distribution (WD) is natural for this purpose, since it is an isometric and invertible operator from the signal space $L^2(\mathbb{R})$ into the time-frequency plane $L^2(\mathbb{R}^2)$. The WD of a signal s is defined as

$$(\mathbf{W}s)(\tau, \nu) = \int s\Big(\tau + \frac{u}{2}\Big)s^*\Big(\tau - \frac{u}{2}\Big)e^{-j2\pi\nu u}\,du.$$

The isometry of the WD follows from Moyal's formula [1], which equates the squared magnitude of the inner product of two signals with the inner product of their respective WDs:[1]

$$|\langle g, h\rangle|^2 = \langle \mathbf{W}g, \mathbf{W}h\rangle. \tag{6}$$

C. Chirplet Transform

Both the STFT and WT fit in the general mold

$$(\mathbf{C}s)(x) = \langle s, \mathbf{M}_x g\rangle$$

where we project the signal to be analyzed $s \in L^2(\mathbb{R})$ onto a set of functions $\{\mathbf{M}_x g\}_{x\in\mathcal{X}}$ obtained by operating on a basic *analyzing function* or *generalized wavelet* $g \in L^2(\mathbb{R})$. The *analysis map* $\mathbf{M}_x$: $L^2(\mathbb{R}) \to L^2(\mathbb{R})$ is a parameterized unitary operator with x from some index set $\mathcal{X}$. From the isometry of the WD, we can write

$$|(\mathbf{C}s)(x)|^2 = |\langle s, \mathbf{M}_x g\rangle|^2 = \langle \mathbf{W}s, \overline{\mathbf{M}}_x\mathbf{W}g\rangle \tag{7}$$

with $\overline{\mathbf{M}}_x$ denoting the action of $\mathbf{M}_x$ on the time-frequency plane $L^2(\mathbb{R}^2)$. This coordinate transformation is defined by

$$\overline{\mathbf{M}}_x = \mathbf{W}\mathbf{M}_x\mathbf{W}^{-1} \tag{8}$$

and maps the subset $\mathcal{W}$ of $L^2(\mathbb{R}^2)$ containing valid WD's into $\mathcal{W}$. Because of the close relationship between $\overline{\mathbf{M}}_x$ and $\mathbf{M}_x$, we will also refer to $\overline{\mathbf{M}}_x$ as the analysis map.

[1] $L^2(\mathbb{R})$ and $L^2(\mathbb{R}^2)$ have inner products $\langle g, h\rangle = \int g(u)h^*(u)\,du$, for $g, h \in L^2(\mathbb{R})$, and $\langle c, d\rangle = \iint c(u, v)d^*(u, v)\,du\,dv$, for $c, d \in L^2(\mathbb{R}^2)$.

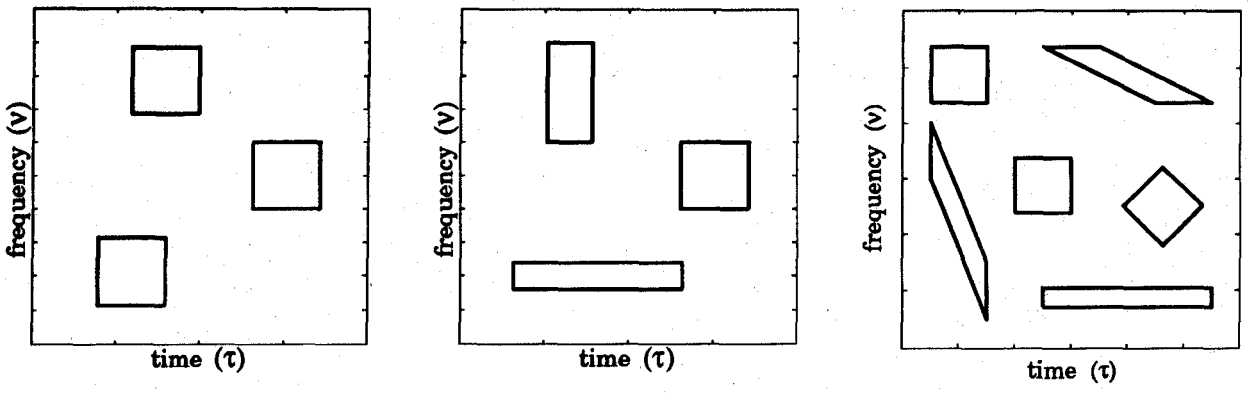

(a) (b) (c)

Fig. 1. Time-frequency transformations underlying the short-time Fourier transform (STFT), the continuous wavelet transform (WT), and the chirplet transform. Each box corresponds to an idealized time-frequency representation of one of the functions onto which the signal is projected. (a) The STFT translates its window function in time-frequency. (b) The WT translates and scales its wavelet function in time-frequency. (c) The chirplet transform can translate, scale, shear, and rotate its generalized wavelet function in time-frequency to match chirping signals.

For the STFT and WT, $\overline{\mathbf{M}}_x^{\mathrm{stft}}$ and $\overline{\mathbf{M}}_x^{\mathrm{wt}}$ correspond to the inverses of (3) and (4), respectively, with $\mathcal{X} = \mathbb{R}^2$. We have

$$[\mathbf{M}_{(t,f)}^{\mathrm{stft}} g](u) = g(u-t)e^{j2\pi fu}$$
$$[\overline{\mathbf{M}}_{(t,f)}^{\mathrm{stft}} \mathbf{W}g](\tau, \nu) = (\mathbf{W}g)(\tau - t, \nu - f)$$
$$[\mathbf{M}_{(t,a)}^{\mathrm{wt}} g](u) = g[e^{-a}(u-t)]$$
$$[\overline{\mathbf{M}}_{(t,a)}^{\mathrm{wt}} \mathbf{W}g](\tau, \nu) = (\mathbf{W}g)[e^{-a}(\tau - t), e^{a}\nu].$$

We obtain the square of the chirplet transform $|(\mathbf{C}^{\mathrm{ct}}s)(x)|^2 = \langle \mathbf{W}s, \overline{\mathbf{M}}_x^{\mathrm{ct}} \mathbf{W}g \rangle$ by plugging into (7) the analysis map

$$(\overline{\mathbf{M}}^{\mathrm{ct}}{}_x \mathbf{W}g)(\tau, \nu) = (\mathbf{W}g)(\tau', \nu') \tag{9}$$

with

$$\begin{bmatrix} \tau' \\ \nu' \end{bmatrix} = A^{-1}\left(\begin{bmatrix} \tau \\ \nu \end{bmatrix} - b \right)$$

and $|A| = 1$. Using the five free parameters of $\overline{\mathbf{M}}_x^{\mathrm{ct}}$ (three from A and two from b), we can translate, scale, and shear $\mathbf{W}g$ in the time-frequency plane (see Fig. 2). In addition, we can rotate $\mathbf{W}g$ using a coordinated scale and shear.

Remark: The WD formulation of the chirplet transform (9) provides a simple rationale for the restriction $|A| = 1$. The determinant $|A|$ controls the time-bandwidth product of the chirplet signal analysis. In a perfect world, this product could be set to any value, so long as the time-frequency uncertainty principle [1] was not violated. However, since the scaled WD $(\mathbf{W}g)(r\tau, c\nu)$ is *not* a valid WD of any function save for the special case $r = c^{-1}$ [11], the map $\mathbf{W}^{-1}\overline{\mathbf{M}}_x^{\mathrm{ct}}\mathbf{W}$—and hence the chirplet transform itself—is not defined for $|A| \neq 1$.

D. Elementary Chirplet Transformations

To exhibit the chirplet transform more explicitly in terms of signals and analyzing wavelets, we can decompose the analysis map (9) into a composition of five distinct one-parameter transformations on the time-frequency plane [9]–[12][2]

$$A^{-1}\left(\begin{bmatrix} \tau \\ \nu \end{bmatrix} - b \right) = \begin{bmatrix} 1 & 0 \\ -q & 1 \end{bmatrix} \begin{bmatrix} 1 & -p \\ 0 & 1 \end{bmatrix} \begin{bmatrix} e^{-a} & 0 \\ 0 & e^{a} \end{bmatrix} \times \left(\begin{bmatrix} \tau \\ \nu \end{bmatrix} - \begin{bmatrix} t \\ 0 \end{bmatrix} - \begin{bmatrix} 0 \\ f \end{bmatrix} \right). \tag{10}$$

[2]We assume that $|A| = 1$ and that the diagonal elements of A^{-1} are nonzero. Otherwise, if a diagonal element of A^{-1} is zero, then a permutation matrix of the form $\left[\begin{smallmatrix} 0 & 1 \\ 1 & 0 \end{smallmatrix}\right]$ must be added to the decomposition (10). This permutation has the simple effect of interchanging the time and frequency coordinates τ and ν.

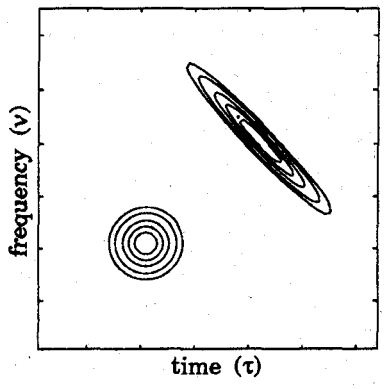

Fig. 2. Wigner distribution (WD) $\mathbf{W}g$ of a Gaussian analyzing wavelet g (bottom left) and $\overline{\mathbf{M}}_x^{\mathrm{ct}}\mathbf{W}g$ transformed according to (9) with $A = \left[\begin{smallmatrix} 2.0 & 0 \\ -2.5 & 0.50 \end{smallmatrix}\right]$ and $b = \left[\begin{smallmatrix} 10 \\ 1.5 \end{smallmatrix}\right]$ (upper right). The corresponding analysis parameters are $x = (10, 1.5, -0.7, 0, -1.25)$; we compute the chirplet transform $|(\mathbf{C}^{\mathrm{ct}}s)(x)|^2$ at x as the inner product of the WD of the signal with $\overline{\mathbf{M}}_x^{\mathrm{ct}}\mathbf{W}g$. The analysis map $\overline{\mathbf{M}}_x^{\mathrm{ct}}$ translates, scales, and shears $\mathbf{W}g$.

The component transformations correspond to (from left to right): shearing in the frequency direction, shearing in the time direction, axis scaling, translation in time, and translation in frequency (recall Fig. 1(c)). Axis scaling and time and frequency translation are familiar from the STFT and WT; the two shear transformations are less well known.

The five parameters controlling these primitive coordinate transformations define an analysis coordinate $x = (t, f, a, p, q)$ in a five-dimensional (5-D) analysis space $\mathcal{X} = \mathbb{R}^5$. The transformation illustrated in Fig. 2, for example, corresponds to the analysis point $x = (10, 1.5, -0.7, 0, -1.25)$.

By applying the inverse of (8) to each primitive component operator in (10), we obtain a corresponding set of unitary component operators of $\mathbf{M}_x^{\mathbf{ct}}$ [3], [9]–[12], as follows:

1) *Time Translation:*

$$(\overline{\mathbf{T}}_t \mathbf{W}g)(\tau, \nu) = (\mathbf{W}g)(\tau - t, \nu)$$
$$(\mathbf{T}_t g)(u) = g(u-t).$$

2) *Frequency Translation:*

$$(\overline{\mathbf{F}}_f \mathbf{W}g)(\tau, \nu) = (\mathbf{W}g)(\tau, \nu - f)$$
$$(\mathbf{F}_f g)(u) = e^{j2\pi fu} g(u).$$

3) *Axis Scaling:*

$$(\overline{\mathbf{A}}_a \mathbf{W} g)(\tau, \nu) = (\mathbf{W} g)(e^{-a}\tau, e^{a}\nu)$$
$$(\mathbf{A}_a g)(u) = e^{-a/2} g(e^{-a}u).$$

4) *Frequency Shear:*

$$(\overline{\mathbf{Q}}_q \mathbf{W} g)(\tau, \nu) = (\mathbf{W} g)(\tau, \nu - q\tau)$$
$$(\mathbf{Q}_q g)(u) = e^{j\pi u^2 q} g(u).$$

5) *Time Shear:*

$$(\overline{\mathbf{P}}_p \mathbf{W} g)(\tau, \nu) = (\mathbf{W} g)(\tau - p\nu, \nu)$$
$$(\mathbf{P}_p g)(u) = (-jp)^{-1/2} e^{j\pi u^2/p} \star g(u).$$

Frequency shear skews the wavelet in the frequency direction in the time-frequency plane through modulation with a linear chirp function. Time shear is obtained through convolution "$\star$" with a linear chirp. (Note that $\lim_{p\to 0} \mathbf{P}_p g = g$.)

Since $\overline{\mathbf{M}}_x^{\mathrm{ct}} = \overline{\mathbf{F}}_f \overline{\mathbf{T}}_t \overline{\mathbf{A}}_a \overline{\mathbf{P}}_p \overline{\mathbf{Q}}_q$ implies that $\mathbf{M}_x^{\mathrm{ct}} = \mathbf{F}_f \mathbf{T}_t \mathbf{A}_a \mathbf{P}_p \mathbf{Q}_q$, we can write the chirplet transform of signal s using generalized wavelet g as

$$|(\mathbf{C}^{\mathrm{ct}} s)(t, f, a, p, q)|^2 = \langle \mathbf{W} s, \overline{\mathbf{F}}_f \overline{\mathbf{T}}_t \overline{\mathbf{A}}_a \overline{\mathbf{P}}_p \overline{\mathbf{Q}}_q \mathbf{W} g \rangle \qquad (11)$$

or

$$(\mathbf{C}^{\mathrm{ct}} s)(t, f, a, p, q) = \langle s, \mathbf{F}_f \mathbf{T}_t \mathbf{A}_a \mathbf{P}_p \mathbf{Q}_q g \rangle$$
$$= (jpe^{a})^{-1/2} \iint s(u) g^{*}[e^{-a}(u-t) - v] \times e^{-j\pi\{2fu + v^2/p + q[e^{-a}(u-t)-v]^2\}} \, du \, dv.$$

By analogy with the spectrogram (the squared magnitude of the STFT) and the scalogram (the squared magnitude of the WT) [2], we could refer to $|\mathbf{C}^{\mathrm{ct}} s|^2$ as the *chirpogram*.

III. Chirplet Subset Transforms

The chirplet concept is more than just a signal transform; within the 5-D chirplet analysis space lie an infinite number of new, lower dimensional signal transforms. For instance, the STFT and WT lie on the 2-D planes parameterized by $x = (t, f, 0, 0, 0)$ and $x = (t, 0, a, 0, 0)$, respectively.

In this section, we go beyond the STFT and WT and construct several new signal transforms, simply by restricting the computation and display of $\mathbf{C}^{\mathrm{ct}} s$ to different analysis subsets. A subset of analysis need not be planar; it could even be curved. Fig. 3 illustrates the action of the chirplet analysis map confined to the tilted analysis plane $x = (t, f, 0, t/2, 0)$.

A. Dispersion Transform

Dispersion artifacts occur in signals acquired from media in which the wave propagation velocity varies with the frequency of the signal. The components of a dispersed signal are tilted in time-frequency—see [15] and [16] for good examples. Fig. 4(a) and (b) illustrates a fundamental limitation of both the STFT and WT for dispersed signals: Since the STFT and WT analysis maps do not tilt the analysis wavelet in time-frequency, the STFT and WT smear dispersed signal components.

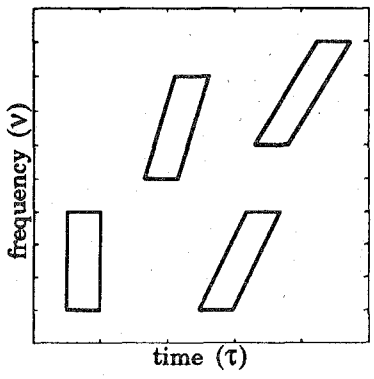

Fig. 3. Dispersion transform. Idealized time-frequency representations of the analysis functions $\mathbf{M}_x^{\mathrm{ct}} g$ for several points lying on the analysis surface $x = (t, f, 0, t/2, 0)$.

The *dispersion transform* [7], [8] evaluates $(\mathbf{C}^{\mathrm{ct}} s)(x)$ at points on the 2-D surface $x = [t, f, p(t, f), 0]$ in the chirplet analysis space

$$(\mathbf{D}s)(t, f) = (\mathbf{C}^{\mathrm{ct}} s)[t, f, 0, p(t, f), 0] = \langle s, \mathbf{F}_f \mathbf{T}_t \mathbf{P}_{p(t,f)} g \rangle$$
$$= [jp(t, f)]^{-1/2} \int s(u) [e^{j\pi u^2/p(t,f)} \star g(u - t)]^{*} \times e^{-j2\pi f u} \, du.$$

The action of the dispersion transform analysis map was shown in Fig. 3 for $p(t, f) = t/2$. Since $p(t, f)$ controls the degree of tilt at the point (t, f) in time-frequency, we call it the *tilt function*.

The dispersion transform is a form of "matched signal processing." If the dispersion characteristics of the medium are known, then a tilt function can be specified to compensate for dispersion and yield a highly concentrated time-frequency representation of the signal. For example, the dispersion transform of the example dispersed signal on the surface $x = (t, f, 0, t/2, 0)$ is shown in Fig. 4(c). Generally, in situations where the dispersion characteristics of the medium are known or can be estimated, the dispersion transform will yield a more concentrated time-frequency representation than either the STFT or the WT.

Conversely, adaptation of the tilt function could be useful in situations where the dispersion characteristics are not known *a priori*. Tuning the tilt function to yield the "most concentrated" representation (several measures of time-frequency concentration are discussed in [17]) results in not only a concentrated time-frequency representation of the signal, but also information on the dispersion characteristics of the medium.

Dispersion transforms based on time-scale-shear surfaces $x = [t, 0, a, p(t, a), 0]$ can be formulated similarly.

B. Nonuniform Filterbanks

The 2-D chirplet analysis surface $x = [t, f, a(f), 0, 0]$ yields a "wavelet-packet-like" time-frequency representation in which the analysis frequency versus analysis bandwidth relationship is unconstrained [14]. This is in contrast to the fixed constant-bandwidth analysis of the STFT and the fixed proportional-bandwidth analysis of the WT.

A nonuniform filterbank allows for closer matching of the transform to signals and systems whose behavior is neither exactly constant nor proportional bandwidth. As an example, consider the human auditory system, in which the analysis is approximately constant bandwidth below about 500 Hz and proportional bandwidth above 500 Hz. Given a wavelet function centered at zero frequency,

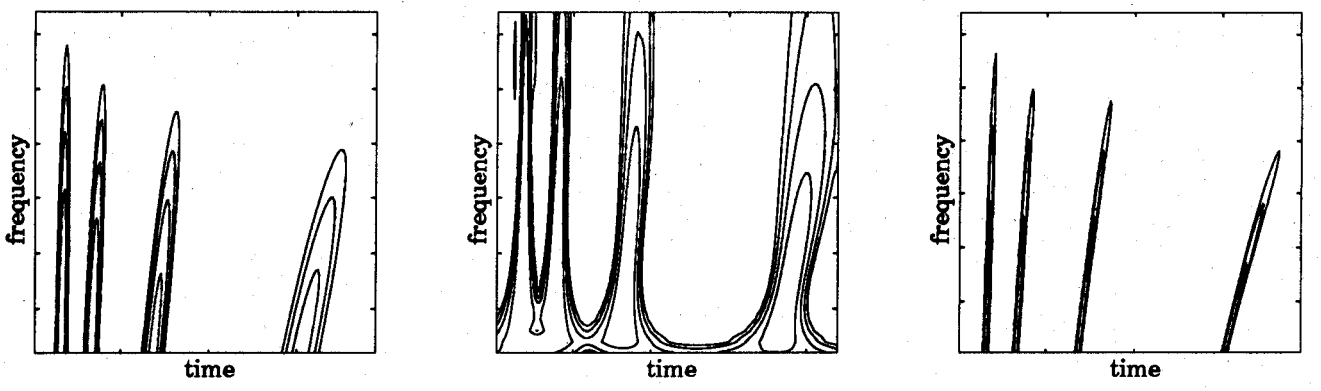

Fig. 4. Comparison of three time-frequency representations of a simulated dispersed signal. (a) STFT. (b) WT. (c) Dispersion transform.

a chirplet analysis surface matching this characteristic is given by

$$x = \begin{cases} (t,\ f,\ 0,\ 0,\ 0), & f \le 500 \text{ Hz} \\ \left(t,\ 500,\ \log \dfrac{500}{f},\ 0,\ 0\right), & f > 500 \text{ Hz}. \end{cases}$$

C. Isometry of Coordinate Analysis Planes

Isometry is a potentially desirable property for a signal transform. Isometry facilitates detection and estimation procedures, in which the inner product of two transforms should equal the inner product of the two signals. Isometry also leads to simple inverse formulas for obtaining the signal corresponding to a given transform.

Generally, the requirement of isometry places constraints on both the transform and the analyzing function. The STFT computed with window function g is isometric with respect to the measure $dt\,df$ [18]

$$\iint (\mathbf{C}^{\text{stft}} s_1)(t,\ f)(\mathbf{C}^{\text{stft}} s_2)^*(t,\ f)\,dt\,df = \|g\|_2^2 \langle s_1,\ s_2\rangle$$

provided $g \in L^2(\mathbb{R})$. Similarly, the WT computed with wavelet g is isometric with respect to the measure $dt\,da$

$$\iint (\mathbf{C}^{\text{wt}} s_1)(t,\ a)(\mathbf{C}^{\text{wt}} s_2)^*(t,\ a)\,dt\,da = \|G\|_{K_1}^2 \langle s_1,\ s_2\rangle$$

provided the wavelet satisfies the admissibility condition $G \in L^2(\mathbb{R}) \cap K_1(\mathbb{R})$ [18].[3] On the contrary, the chirplet transform is not isometric with respect to its natural (Haar) measure $dt\,df\,da\,dp\,dq$. In fact, it is not even square integrable, as in

$$\iiiii |(\mathbf{C}^{\text{ct}} s)(t,\ f,\ a,\ p,\ q)|^2\,dt\,df\,da\,dp\,dq = \|s\|_2^2\,\|g\|_2^2 \iiint da\,dp\,dq = \infty.$$

When properly restricted to an appropriate analysis subset, the chirplet transform gains the isometry property. (The 2-D analysis planes corresponding to the STFT and WT supply two obvious examples.) In Table I, we summarize the isometry properties of the transforms generated by the 2-D planes lying along the coordinate axes in $\mathbb{R}^5$ [8]. These planes are parameterized by all possible *conjugate* combinations of two of the five chirplet parameters. We call two chirplet parameters conjugate if the restricted analysis map $\overline{\mathbf{M}}_x$ maps $\mathbb{R}^2$ (the conjugate parameter space) onto $\mathbb{R}^2$ (the time-frequency plane). (In words, $\overline{\mathbf{M}}_x$ must reach all points in the time-frequency plane.) Not all combinations of the five chirplet parameters are conjugate. For example, time-shift t and time-shear p are not conjugate, because both are capable of displacements only in the time direction.

[3] Capital letters denote Fourier transforms, and $\|g\|_2^2 = \langle g,\ g\rangle$ denotes the usual $L^2(\mathbb{R})$ norm. In addition, define the weighted norm $\|h\|_{K_r}^2 = \int |h(u)|^2\,|u|^{-r}\,du$, $r \in \mathbb{R}$, and corresponding weighted Hilbert space $K_r(\mathbb{R}) = \{h\colon \|h\|_{K_r} < \infty\}$. Note that $K_0(\mathbb{R}) = L^2(\mathbb{R})$.

TABLE I

FIVE 2-D COORDINATE PLANE TRANSFORMS INHABITING THE 5-D CHIRPLET ANALYSIS SPACE. SUMMARIZED ARE THE ANALYSIS PLANE OF DEFINITION, THE SIGNAL SPACE FROM WHICH THE TRANSFORMS ARE ISOMETRIES (THEY ARE ALL ISOMETRIES *INTO* SUBSETS OF $L^2(\mathbb{R}^2)$), AND THE ADMISSIBILITY CONDITIONS ON THE WAVELET g OR ITS FOURIER TRANSFORM G FOR THE TRANSFORM TO BE ISOMETRIC. WE USE THE ABBREVIATIONS L^2 FOR $L^2(\mathbb{R})$ AND K_r FOR $K_r(\mathbb{R})$ AND ASSUME THAT THE NATURAL LEBESQUE MEASURE $du\,dv$ IS EMPLOYED IN THE TRANSFORM SPACE $L^2(\mathbb{R}^2)$.

Transform	Plane	Signal space	Admissibility Condition
STFT	(t,f)	L^2	$g \in L^2$
WT	(t,a)	L^2	$G \in L^2 \cap K_1$
	(f,a)	L^2	$g \in L^2 \cap K_1$
Scale and shear	(a,p)	L^2	$G \in L^2 \cap K_2$
	(a,q)	L^2	$g \in L^2 \cap K_2$
Translation and shear	(t,q)	L^2	$g \in L^2 \cap K_1$
	(f,p)	L^2	$G \in L^2 \cap K_1$
Double shear	(p,q)	$K_1 \cap L^2$	$G \in L^2 \cap K_1$

For each coordinate plane, isometry places an admissibility constraint on the generalized wavelet g (see Table I). We demonstrate only for the $(a,\ p)$ scale-shear transform case; the others are similar. Using the WD and Moyal's formula (6), we have

$$\begin{aligned} &\|(\mathbf{C}^{\text{ct}} s)(a,\ p)\|_2^2 \\ &= \iint |(\mathbf{C}^{\text{ct}} s)(a,\ p)|^2\,da\,dp = \iint |\langle s,\ \mathbf{A}_a \mathbf{P}_p g\rangle|^2\,da\,dp \\ &= \iint \langle \mathbf{W}s,\ \overline{\mathbf{A}}_a \overline{\mathbf{P}}_p \mathbf{W} g\rangle\,da\,dp \\ &= \iiii (\mathbf{W}s)(\tau,\ \nu)(\mathbf{W}g)(e^{-a}\tau - pe^{a}\nu,\ e^{a}\nu)d\tau\,d\nu\,da\,dp \\ &= \iiii (\mathbf{W}s)(\tau,\ \nu)(\mathbf{W}g)(u,\ v)v^{-2}\,d\tau\,d\nu\,du\,dv \qquad (12) \\ &= \iint (\mathbf{W}s)(\tau,\ \nu)\,d\tau\,d\nu \int \left[\int (\mathbf{W}g)(u,\ v)\,du\right] v^{-2}\,dv \\ &= \|s\|_2^2 \int |G(v)|^2 v^{-2}\,dv \;=\; \|s\|_2^2\,\|G\|_{K_2}^2. \qquad (13) \end{aligned}$$

Therefore, the $(a,\ p)$ transform is isometric if $G \in L^2(\mathbb{R}) \cap K_2(\mathbb{R})$ with unit K_2 norm. To obtain (12), we made the change of variables

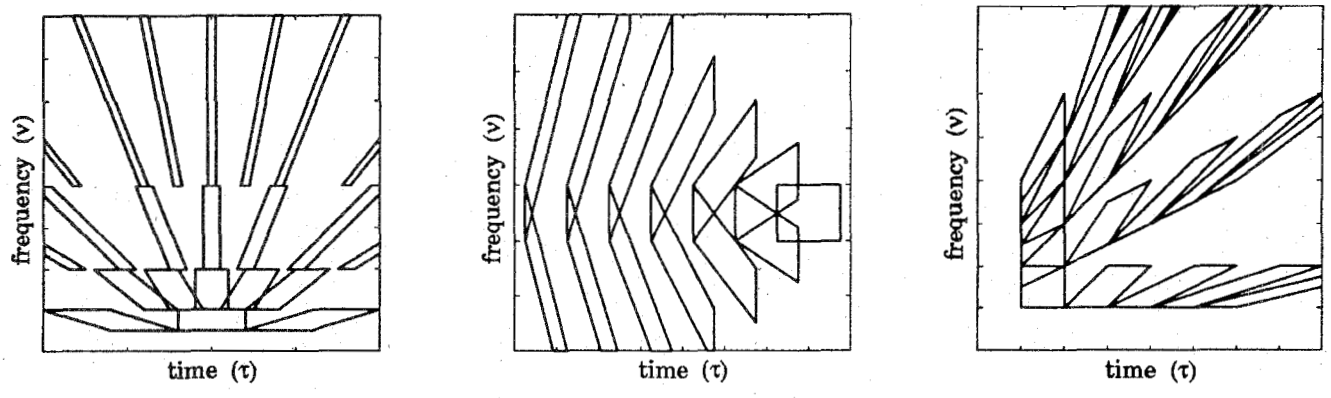

Fig. 5. Time-frequency transformations underlying the new transforms from Table I: (a) the (a, p) scale-shear transform; (b) the (t, q) time-shear transform; and (c) the (p, q) double shear transform. To obtain the transformations underlying the (a, q) and (f, p) transforms, rotate (a) and (b) by 90°.

$u = e^{-a}\tau - pe^{a}\nu$, $v = e^{a}\nu$; to obtain (13), we used the marginal property $\int (\mathbf{W}h)(u, v)\, du = |H(v)|^2$ of the WD [1].

Fig. 5 illustrates the action of the analysis map on the time-frequency plane for three of the new transforms appearing in Table I. The scale-shear, translation-shear, and double-shear transforms each involve either modulation or convolution with linear chirp functions.

D. New Bilinear Distribution Classes

As an added bonus, our energetic derivation of the chirplet transform permits a straightforward derivation of quadratic distributions extending STFT's and WT's. In particular, replacing $\mathbf{W}g$ in (11) with an arbitrary 2-D kernel function Φ yields a class of bilinear chirplet distributions

$$(\mathbf{Z}s)(x) = \langle \mathbf{W}s, \overline{\mathbf{F}}_f \overline{\mathbf{T}}_t \overline{\mathbf{A}}_a \overline{\mathbf{P}}_p \overline{\mathbf{Q}}_q \Phi \rangle$$

with a continuously variable time-frequency-scale-shear smoothing tradeoff. This class of transforms is very large, and contains the distributions of both Cohen's class [1] and the affine class [2].

IV. Discussion and Conclusions

In addition to generalizing and providing a unifying framework for studying existing linear signal representations like the STFT and the WT, the chirplet transform provides a systematic method for designing new signal representations with interesting and useful properties. The example transforms presented in Section III indicate that there is something to be gained from stepping out of the strict time-frequency or time-scale paradigms. Furthermore, these examples merely scratch the surface of possible linear signal representations that can be derived using the chirplet transform—there are as many different representations in the chirplet space as there are subsets in $\mathbb{R}^5$.

The chirplet concept also provides a convenient framework for formulating adaptive or signal-dependent time-frequency or time-scale representations. In this case, the three extra degrees of freedom can be tuned to optimize some measure of performance in the representation. For example, both the adaptive-window STFT of Jones and Parks [19] and the adaptive bowtie transform of Mann and Haykin [5] can be formulated as finding the 2-D surface in the 5-D chirplet space such that $\mathbf{C}^{\mathrm{ct}}s$ evaluated along that surface is maximally concentrated.

Many connections exist between the affine transformation (5), the analysis map $\mathbf{M}_x^{\mathrm{ct}}$ of the chirplet transform, and the representation theory of the *extended metaplectic group* [9]. This group contains as subgroups both the Weyl–Heisenberg group, which spawns the STFT, and the 1-D affine group, which spawns the WT and the (a, p) and (a, q) scale-shear transforms [7], [8], [20]. The utility of group theoretic constructs for defining new transforms is limited, however, because many interesting transforms (the (t, q) time-shear transform represents only one example) correspond to surfaces in the chirplet analysis space that lack a group structure.

The STFT and WT share the attractive property that both can be discretized to form orthogonal bases and frames for $L^2(\mathbb{R})$. While a general theory of discrete chirplet transforms has yet to be discovered, a successful discretization has been performed along the (a, p) scale and time-shear plane in the chirplet space to yield the *fan* bases [21], [22]. Interestingly, this orthonormal basis represents signals without using any translations of the mother wavelet function.

Finally, note that the generalization of the STFT and WT does not have to stop at 2-D affine transformations such as (5). In addition to shearing and rotating functions in time-frequency, transforms based on higher dimensional analysis spaces (using quadratic frequency modulations, $e^{j\kappa u^3}$, for example) will manipulate their *curvature* [22].

Acknowledgment

The authors acknowledge S. Mann and S. Haykin for discussions related to the chirplet transform and thank M. Bergvelt and G. Folland for numerous helpful comments regarding the metaplectic representation.

References

[1] L. Cohen, *Time-Frequency Analysis.* Englewood Cliffs, NJ: Prentice-Hall, 1995.

[2] O. Rioul and P. Flandrin, "Time-scale energy distributions: A general class extending wavelet transforms," *IEEE Trans. Signal Processing,* vol. 40, pp. 1746–1757, July 1992.

[3] A. Grossman and T. Paul, "Wave functions on subgroups of the group of affine canonical transformations," in *Lecture Notes in Physics no. 211: Resonances—Models and Phenomena,* L. Strein, Ed. New York: Springer-Verlag, 1984, pp. 128–138.

[4] A. Berthon, "Operator groups and ambiguity functions in signal processing," in *Wavelets: Time-Frequency Methods and Phase Space,* J. M. Combes, A. Grossman, and P. Tchamitchian, Eds. New York: Springer-Verlag, 1989, pp. 172–180.

[5] S. Mann and S. Haykin, "The chirplet transform: Physical considerations," *IEEE Trans. Signal Processing,* vol. 43, pp. 2745–2761, Nov. 1995.

[6] S. Mann, R. G. Baraniuk, S. Haykin, and D. L. Jones, "The chirplet transform," *IEEE Trans. Signal Processing,* submitted, 1992.

[7] R. G. Baraniuk and D. L. Jones, "New dimensions in wavelet analysis," in *Proc. IEEE Int. Conf. Acoust., Speech, Signal Processing: ICASSP '92,* vol. V, 1992, pp. 137–140.

[8] R. G. Baraniuk, "Shear madness: Signal-dependent and metaplectic time-frequency representations," Ph.D. dissertation, Dept. Electr. Comput. Eng., Univ. Illinois at Urbana-Champaign, 1992.
[9] G. B. Folland, *Harmonic Analysis in Phase Space.* Princeton, NJ: Princeton Univ. Press, 1989.
[10] A. Papoulis, *Signal Analysis.* New York: McGraw-Hill, 1977.
[11] A. J. E. M. Janssen, "On the locus and spread of pseudo-density functions in the time-frequency plane," *Philips J. Res.,* vol. 37, no. 3, pp. 79–110, 1982.
[12] D. L. Jones and T. W. Parks, "Time-frequency window leakage in the short-time Fourier transform," *Circuits, Signals, Syst.,* vol. 6, no. 3, pp. 263–286, 1987.
[13] W. Schempp, *Harmonic Analysis on the Heisenberg Nilpotent Lie Group.* Harlow, England: Longman, 1986.
[14] B. Torrésani, "Wavelets associated with representations of the affine Weyl–Heisenberg group," *J. Math. Phys.,* vol. 32, no. 5, pp. 1273–1279, 1991.
[15] J. P. Sessarego, J. Sageloli, P. Flandrin, and M. Zakharia, "Time-frequency analysis of signals related to scattering problems in acoustics," in *Wavelets: Time-Frequency Methods and Phase Space,* J. M. Combes, A. Grossman, and P. Tchamitchian, Eds. New York: Springer-Verlag, 1989, pp. 147–153.
[16] A. K. Booer, J. Chambers, and I. M. Mason, "Fast numerical algorithm for the recompression of dispersed time signals," *IEE Electr. Lett.,* vol. 13, pp. 453–455, Aug. 4, 1977.
[17] R. G. Baraniuk, P. Flandrin, and O. Michel, "Measuring time-frequency information content using the Rényi entropies," preprint, 1995.
[18] A. Grossman, J. Morlet, and T. Paul, "Transforms associated with square-integrable group representations. Part 1. General results," *J. Math. Phys.,* vol. 26, pp. 2473–2479, Oct. 1985.
[19] D. L. Jones and T. W. Parks, "A high resolution data-adaptive time-frequency representation," *IEEE Trans. Acoust., Speech, Signal Processing,* vol. 38, pp. 2127–2135, Dec. 1990.
[20] T. Paul, "Functions analytic on the half-plane as quantum mechanical states," *J. Math. Phys.,* vol. 25, pp. 3252–3263, Nov. 1984.
[21] R. G. Baraniuk and D. L. Jones, "Shear madness: New orthonormal bases and frames using chirp functions," *IEEE Trans. Signal Processing,* vol. 41, pp. 3543–3548, Dec. 1993.
[22] ——, "Unitary equivalence: A new twist on signal processing," *IEEE Trans. Signal Processing,* vol. 43, pp. 2269–2282, Oct. 1995.

Efficient Implementation of Koilpillai–Vaidyanathan Pseudo Quadrature Mirror Filter (PQMF) Banks

Xiang Wei, Martyn J. Shaw, and Martin R. Varley

***Abstract*— An efficient implementation algorithm for the Koilpillai–Vaidyanathan pseudo quadrature mirror filter (KVPQMF) bank, which is useful in audio compression schemes, is presented. The implementation employs a polyphase system with discrete cosine transforms (DCT's). Theoretical and practical results show a typical saving in computational load of 82% over the direct implementation.**

I. Introduction

Subband coding has been widely used for audio compression [1]. By means of filter banks, it splits the signal into M frequency channels, encodes and decodes each channel, and reconstructs the signal. Typically, pseudo quadrature mirror filter (PQMF) banks are often employed for subband coding of audio signals because of their comparative low costs of design and implementation, low latency, and satisfactory reconstruction quality [2]. Koilpillai and Vaidyanathan [3] proposed a spectral factorization approach to the PQMF design, which has an advantage over others in that the design of the prototype filter is very easy and efficient since no optimization is involved; rather, it is found by simply factorizing a $2M$th band filter. This is relatively simple to carry out using Kaiser window, FFT, and Levinson–Durbin algorithms [3]. Our experiences show that it is easy to obtain high stopband attenuation (≈ -100 dB) and small aliasing (≈ -100 dB). The total magnitude response is flat with a reasonably small distortion level (≈ -50 dB) in the region $\varepsilon \leq \omega \leq \pi - \varepsilon$, where $0 < \varepsilon < \pi/2M$. These specifications are particularly attractive for audio coding. The filters do not have linear phase, but the overall transfer function has a linear phase. In a recent paper [4], a filter bank design method for less flatness distortion and a linear-phase prototype filter was proposed, but the prototype filter design relies on optimization and demands more complexity.

The authors are currently using the Koilpillai–Vaidyanathan PQMF (KVPQMF) bank for work on subband coding of digital audio signals [5], and this has been the motivation for developing a fast implementation.

The structure of the KVPQMF bank is the same as the conventional PQMF bank. The difference lies in the derivation of the analysis and synthesis filters. From a prototype filter $h(n)$ of length N, where $(N-1) = mM$ and m is an integer, the kth channel analysis filter coefficients $h_k(n)$ and synthesis filter coefficients $g_k(n)$ are found as (1), which appears at the bottom of the next page, where

$$g_k(n) = h_k(N-1-n) \qquad \begin{matrix} 0 \leq k \leq M-1 \\ 0 \leq k \leq M-1 \end{matrix} \tag{2}$$

and where M is the number of channels, and θ_k is an arbitrary angle [3]. Aliasing may occur in the reconstructed signal, but with certain constraints on the θ_k, the significant aliasing terms are cancelled. Not losing generality, we adopt the constraints on angles as [3]

$$\theta_{k+1} = \pi/2 - \theta_k, \qquad 0 \leq k \leq M-2. \tag{3}$$

The total magnitude response is flat except around 0 and π, where some peaks and troughs appear, but they can be minimized by optimizing the single parameter θ_0 [3].

It has been shown that by taking advantage of the cosine-modulated structure, the implementation of conventional PQMF banks can be made efficient by deriving a polyphase structure employing discrete cosine transforms (DCT's) [6], [7]. In [3], comparisons were made between KVPQMF banks and conventional PQMF banks, and it was stated that the KVPQMF banks do not possess this property. In this paper, it will be shown that this is not true, and the work in [6] and [7] is extended to KVPQMF banks. The method relies on a polyphase structure that is suitable for KVPQMF banks by employing M-point DCT's and inverse DCT's (IDCT's). It is shown that efficient implementation has a considerable saving in computational load over the direct method. The saving increases with the number of channels and the length of prototype filter. Programs written in the C language running on an HP workstation shows that the saving in time is about 82% for 32-channel KVPQMF banks of filter length $N = 225$.

In the following sections, it is explained how the polyphase structure of the analysis and synthesis filter banks is derived. The block diagram of the efficient implementation is shown. Finally,

Manuscript received April 7, 1995; revised June 10, 1996. The associate editor coordinating the review of this paper and approving it for publication was Prof. Tyseer Aboulansr.

The authors are with the Department of Electrical and Electronic Engineering, University of Central Lancashire, Preston PR1 2HE, United Kingdom.

Publisher Item Identifier S 1053-587X(96)08228-1.